



Film Cooling Flow Effects on Post-Combustor Trace Chemistry

Thomas Wey
Taitech, Inc., Beavercreek, Ohio

Nan-Suey Liu
Glenn Research Center, Cleveland, Ohio

The NASA STI Program Office . . . in Profile

Since its founding, NASA has been dedicated to the advancement of aeronautics and space science. The NASA Scientific and Technical Information (STI) Program Office plays a key part in helping NASA maintain this important role.

The NASA STI Program Office is operated by Langley Research Center, the Lead Center for NASA's scientific and technical information. The NASA STI Program Office provides access to the NASA STI Database, the largest collection of aeronautical and space science STI in the world. The Program Office is also NASA's institutional mechanism for disseminating the results of its research and development activities. These results are published by NASA in the NASA STI Report Series, which includes the following report types:

- **TECHNICAL PUBLICATION.** Reports of completed research or a major significant phase of research that present the results of NASA programs and include extensive data or theoretical analysis. Includes compilations of significant scientific and technical data and information deemed to be of continuing reference value. NASA's counterpart of peer-reviewed formal professional papers but has less stringent limitations on manuscript length and extent of graphic presentations.
- **TECHNICAL MEMORANDUM.** Scientific and technical findings that are preliminary or of specialized interest, e.g., quick release reports, working papers, and bibliographies that contain minimal annotation. Does not contain extensive analysis.
- **CONTRACTOR REPORT.** Scientific and technical findings by NASA-sponsored contractors and grantees.

- **CONFERENCE PUBLICATION.** Collected papers from scientific and technical conferences, symposia, seminars, or other meetings sponsored or cosponsored by NASA.
- **SPECIAL PUBLICATION.** Scientific, technical, or historical information from NASA programs, projects, and missions, often concerned with subjects having substantial public interest.
- **TECHNICAL TRANSLATION.** English-language translations of foreign scientific and technical material pertinent to NASA's mission.

Specialized services that complement the STI Program Office's diverse offerings include creating custom thesauri, building customized databases, organizing and publishing research results . . . even providing videos.

For more information about the NASA STI Program Office, see the following:

- Access the NASA STI Program Home Page at <http://www.sti.nasa.gov>
- E-mail your question via the Internet to help@sti.nasa.gov
- Fax your question to the NASA Access Help Desk at 301-621-0134
- Telephone the NASA Access Help Desk at 301-621-0390
- Write to:
NASA Access Help Desk
NASA Center for Aerospace Information
7121 Standard Drive
Hanover, MD 21076



Film Cooling Flow Effects on Post-Combustor Trace Chemistry

Thomas Wey
Taitech, Inc., Beavercreek, Ohio

Nan-Suey Liu
Glenn Research Center, Cleveland, Ohio

National Aeronautics and
Space Administration

Glenn Research Center

Acknowledgments

The geometry of the turbine vane and Version 3.1 (May 1999) of the GLENN-HT, from which we extended into CGLENN-HT, are provided to us by Dr. James Heidmann, NASA Glenn Research Center, Turbine Branch.

This report is a formal draft or working paper, intended to solicit comments and ideas from a technical peer group.

Available from

NASA Center for Aerospace Information
7121 Standard Drive
Hanover, MD 21076

National Technical Information Service
5285 Port Royal Road
Springfield, VA 22100

Available electronically at <http://gltrs.grc.nasa.gov>

Film Cooling Flow Effects On Post-Combustor Trace Chemistry

Thomas Wey
Taitech, Inc.
Beavercreek, Ohio 45430

Nan-Suey Liu
National Aeronautics and Space Administration
Glenn Research Center
Cleveland, Ohio 44135

1 Introduction

Film cooling injection is widely applied in the thermal design of turbomachinery, as it contributes to achieve higher operating temperature conditions of modern gas turbines, and to meet the requirements for reliability and life cycles. It is a significant part of the high-pressure turbine system. The film cooling injection, however, interacts with the main flow and is susceptible to have an influence on the aerodynamic performance of the cooled components, and through that may cause a penalty on the overall efficiency of the gas turbine. The main reasons are the loss of total pressure resulting from mixing the cooling air with the mainstream and the reduction of the gas stagnation temperature at the exit of the combustion chamber to a lower value at the exit of nozzle guide vane. In addition, the impact of the injected air on the evolution of the trace species of the hot gas is not yet quite clear. This work computationally investigates the film cooling influence on post-combustor trace chemistry, as trace species in aircraft exhaust affect climate and ozone.

2 Codes used

CGLENN-HT and NCC are selected as the primary working codes, while CNEWT-GRC is used as a reference. A description of these codes can be found in Ref. [1]

3 Geometry and mesh

The turbine vane of this study is based on an Allied-Signal film-cooled engine design [2]. An enlarged view of the cooling hole meshes in the leading edge region is shown in Figure 1. In the present study, a two-dimensional representation of the cooling holes is used, i.e. a slot is used to replace a row of holes. The plenums are also not included in the computational domain.

An overset/Chimera grid is generated for both CGLENN-HT and NCC. This grid consists of two component grids: a hyperbolic marching grid generator in T3D is used to generate an O grid around the vane, while an algebraic H grid is generated to cover the flow passage. OVERGC[3], acronym of overset grid communicator, is then used to build grid interfaces between these two component grids. Furthermore, FPLOT is used to convert the composite grids resulting from OVERGC to the format of overset unstructured grids for NCC, as well as the format of overset structured grids for CGLENN-HT. FPLOT is also used to tag boundary elements and fluid elements for the NCC. The final composite grid is shown in Figure 2. The positions and directions of the cooling air slots are indicated in Figure 3

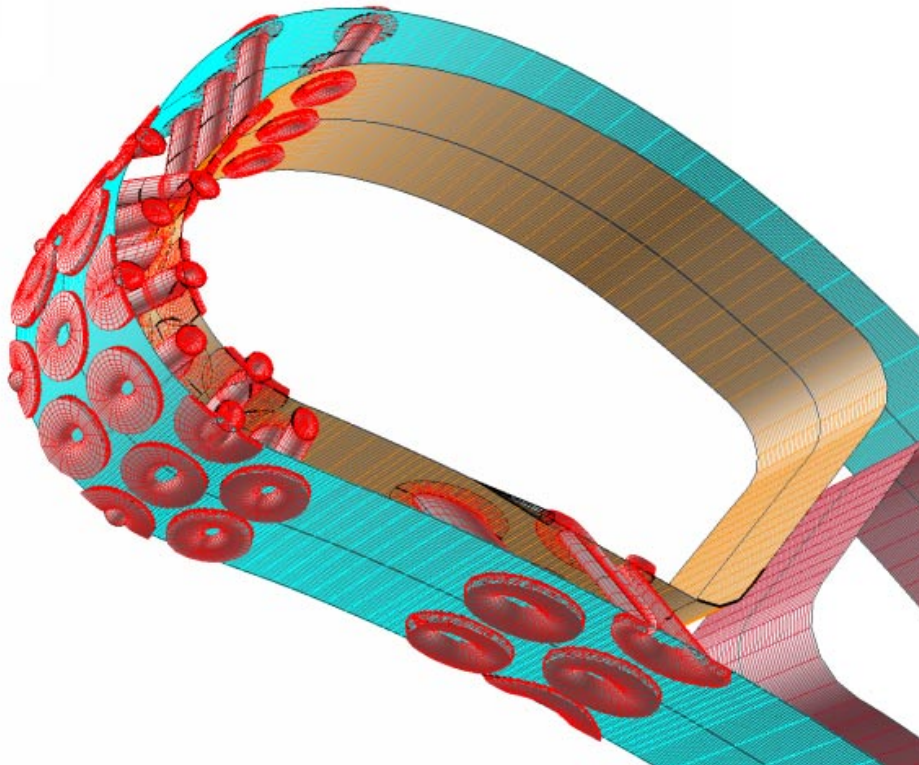


Figure 1: The leading edge region of a three dimensional mesh of the cooling holes

A TURBINE VANE WITH 12 COOLING SLOTS

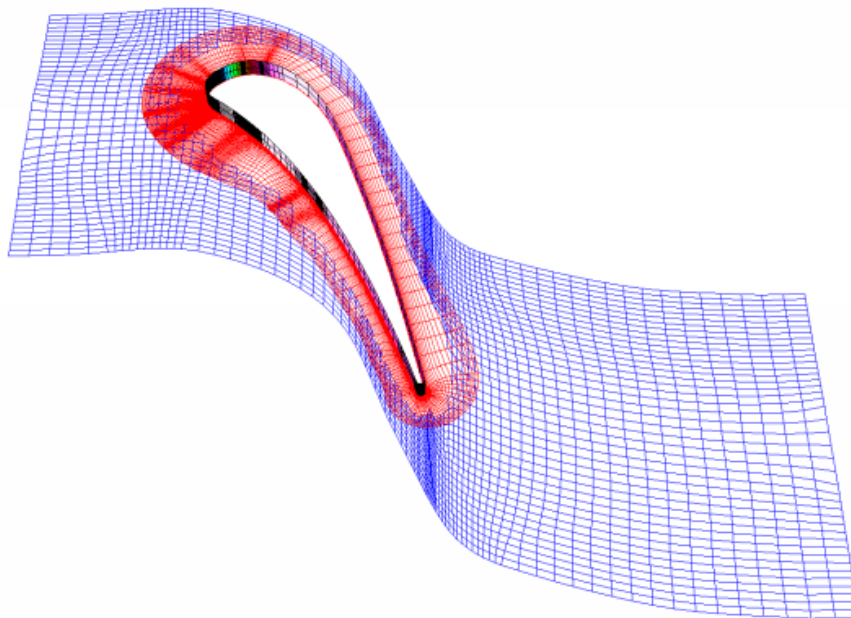


Figure 2: A two-block overset grid around the vane. (Thickness of vane is about .01 meter.)

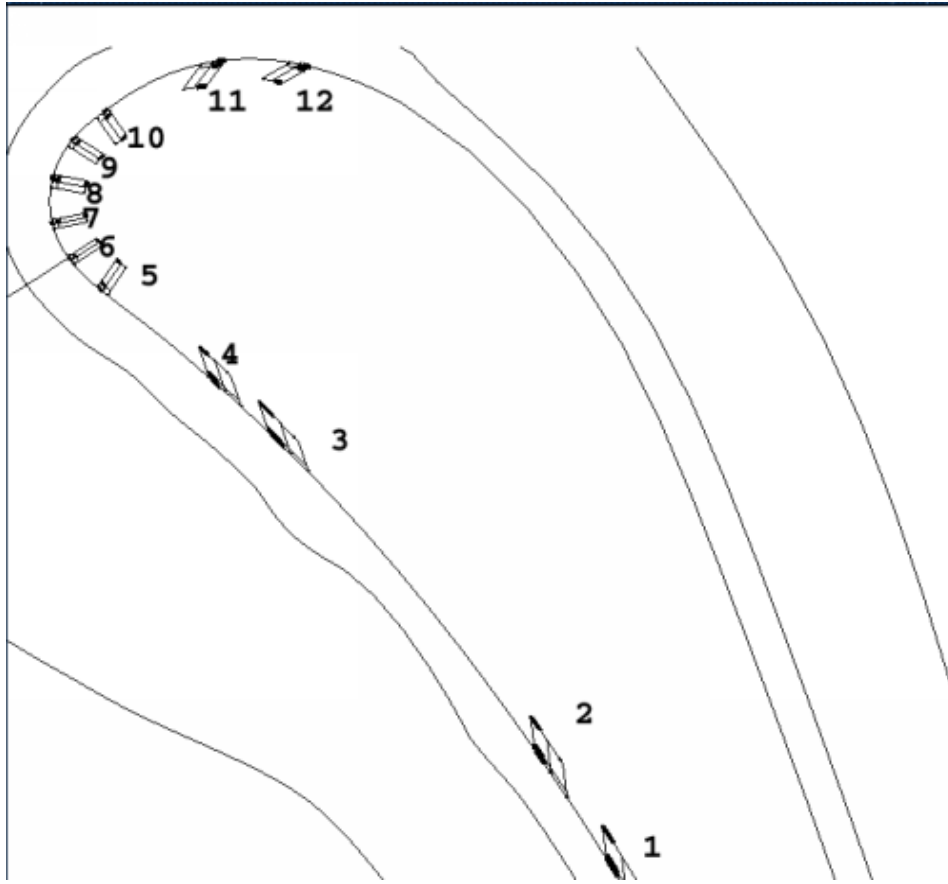


Figure 3: The positions and directions of the cooling air slots.

Slot no.	$\frac{\dot{M}}{A} (\frac{kg}{s \cdot m^2})$	flow angle (degree)
1	110.46	-65.5
2	97.38	-62.9
3	130.54	-63.8
4	115.52	-61.4
5	94.52	186.2
6	186.28	182.7
7	202.12	180.9
8	210.6	179.1
9	251.68	177.1
10	128.76	175.6
11	159.66	44.5
12	171.26	47.0

Table 1: Film-cooling inlet flow parameters

4 Boundary conditions

At the mainstream inlet, the total pressure of the mainstream hot gas is set to be 1629080 N/M^2 ; the total temperature is 1644.42 K ; and the specific heat at constant pressure is 1138 J/kgK . Following standard practice the value for the turbulence intensity is 4% of the computed inlet normal velocity, while the turbulence length scale at the inlet is set to be .05 m . At the exit, the static pressure is set to be 938350.08 N/M^2 , i.e. 57.6% of the inlet total pressure. The surface temperature of the vane is 1151 K .

The coolant mass flow is about five percent of the mainstream hot gas mass flow. Cooling air at a total temperature of 822.1 K is discharged into the mainstream through 12 slots along the vane surface to form a cooling film. The specifications of the coolant mass flux and discharged angle at each slot are listed in Table 1. The composition of the species for the inlet mainstream gas as well as the cooling air are listed in Table 2. The trace chemistry mechanism used is the one reported in [4]. It has twenty five species and seventy four reaction steps.

	Species	Mass fraction at main inlet	Mass fraction of cooling air
1	C(S)	.2437335E-05	0
2	H2	.2327455E-07	0
3	O2	.1438427E+00	0.21
4	H2O	.2986734E-01	0.01
5	O	.1098798E-05	0
6	H	.4135477E-09	0
7	OH	.4075543E-04	0
8	HO2	.7921337E-06	0
9	H2O2	.2097706E-07	0
10	CO	.1947870E-03	0
11	CO2	.7671610E-01	0.02
12	N	.0000000E+00	0
13	N2	.7491807E+00	0.76
14	NO	.1098798E-03	0
15	NO2	.1877946E-04	0
16	HNO	.1048853E-08	0
17	HONO	.1388482E-06	0
18	N2O	.0000000E+00	0
19	NO3	.4744811E-10	0
20	HNO3	.4505073E-09	0
21	SO	.3026690E-10	0
22	SO2	.2377400E-04	0
23	SO3	.6762604E-06	0
24	HSO3	.1678165E-09	0
25	H2SO4	.2727018E-10	0

Table 2: Species distributions at the inlet of the and cooling air

5 Evaluation of transport properties

Transport properties are evaluated differently in different codes, they are summarized as the following three options.

1. Option 1 — The temperature is iteratively computed from the static enthalpy of the gas mixture, h , and the specific heat at constant pressure of the gas mixture, C_p . In addition, the gas constant of the mixture, the specific heat at constant pressure of the gas mixture, laminar viscosity of the mixture and thermal conductivity of the mixture are all functions of species mass fractions and the temperature.
2. Option 2 — The temperature is computed from the enthalpy of the gas mixture, h and a constant C_p . Gas constant of the mixture, specific heat at constant pressure of the gas mixture, C_p , laminar viscosity of the mixture and thermal conductivity of the mixture are all constants which are either user specified parameters or computed via other parameters such as Prandtl number.
3. Option 3 — The gas constant of the mixture and the specific heat at constant pressure of the gas mixture, C_p , are constants provided by the users. The laminar viscosity of the mixture is calculated using a power-law for its dependence on temperature.. The thermal conductivity of the mixture is computed through Prandtl number and C_p . The temperature is computed from the equation of state.

6 Computational results

Five sets of computed results are assembled together to show the difference due to various codes and cooling air injection. They are: (1) CGLENN-HT using option 3 without cooling air, (2) NCC using option 1 without cooling air, (3) CNEWT-GRC using option 2 without cooling air, (4) CGLENN-HT using option 3 with cooling air, and (5) NCC using option 1 with cooling air. Numerical simulation without film cooling represents the first step in the analysis. Its converged solution is then used as the initial condition for the film cooling computation. Data reduction has been performed to get one dimensional distribution along the axis of the flow path by averaging the CFD results.

The pressure contours of the five cases are shown in Figure 4. The area-averaged pressure distributions along the axis of the flow path are given in Figure 5. These results suggest that the differences of the pressure distribution among the five cases are minimal.

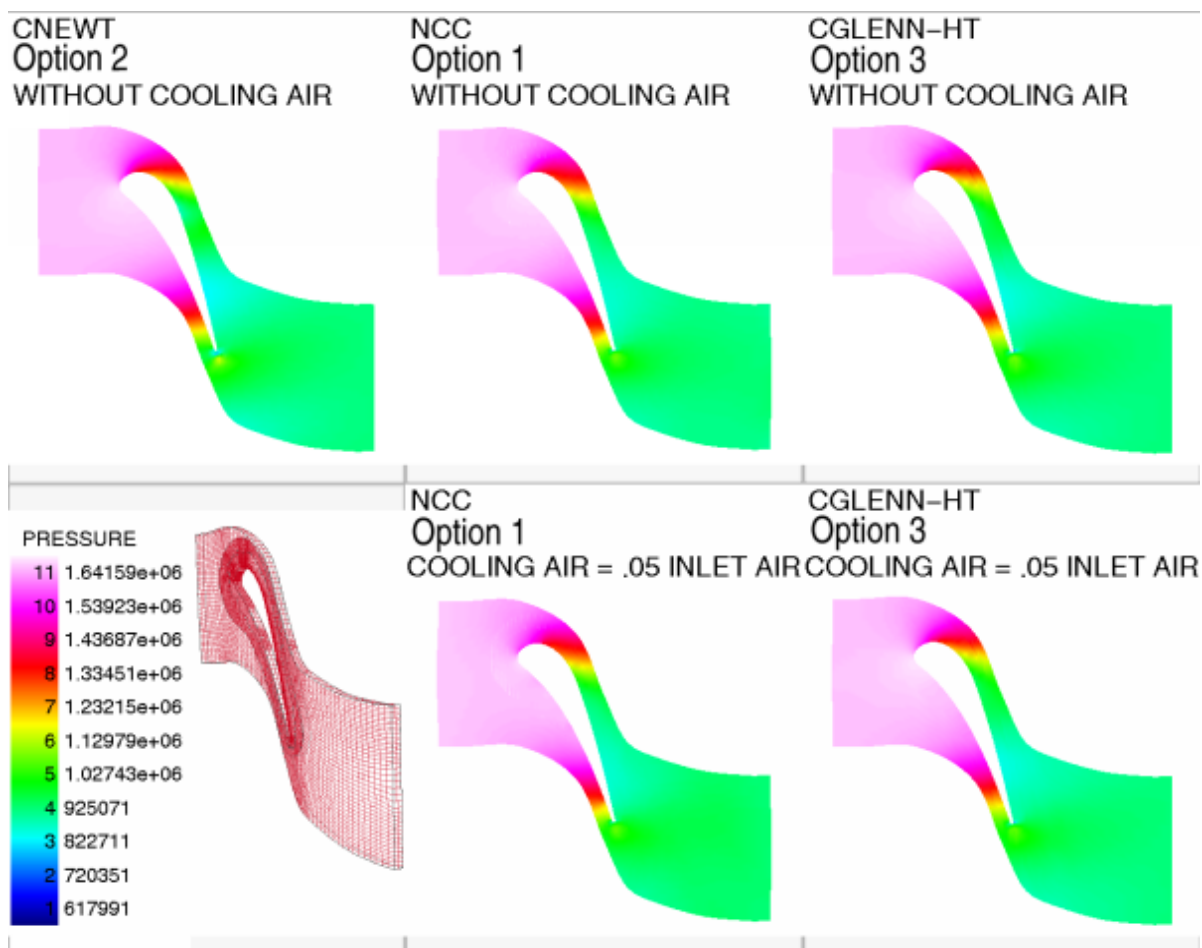


Figure 4: Comparison of pressure distributions.

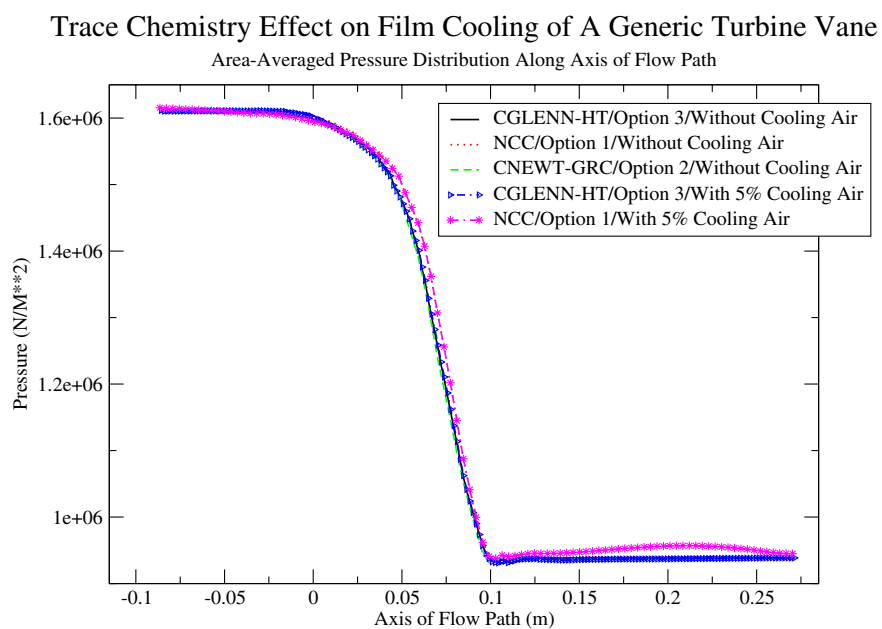


Figure 5: Comparison of area-averaged pressure distributions along the axis of flow path.

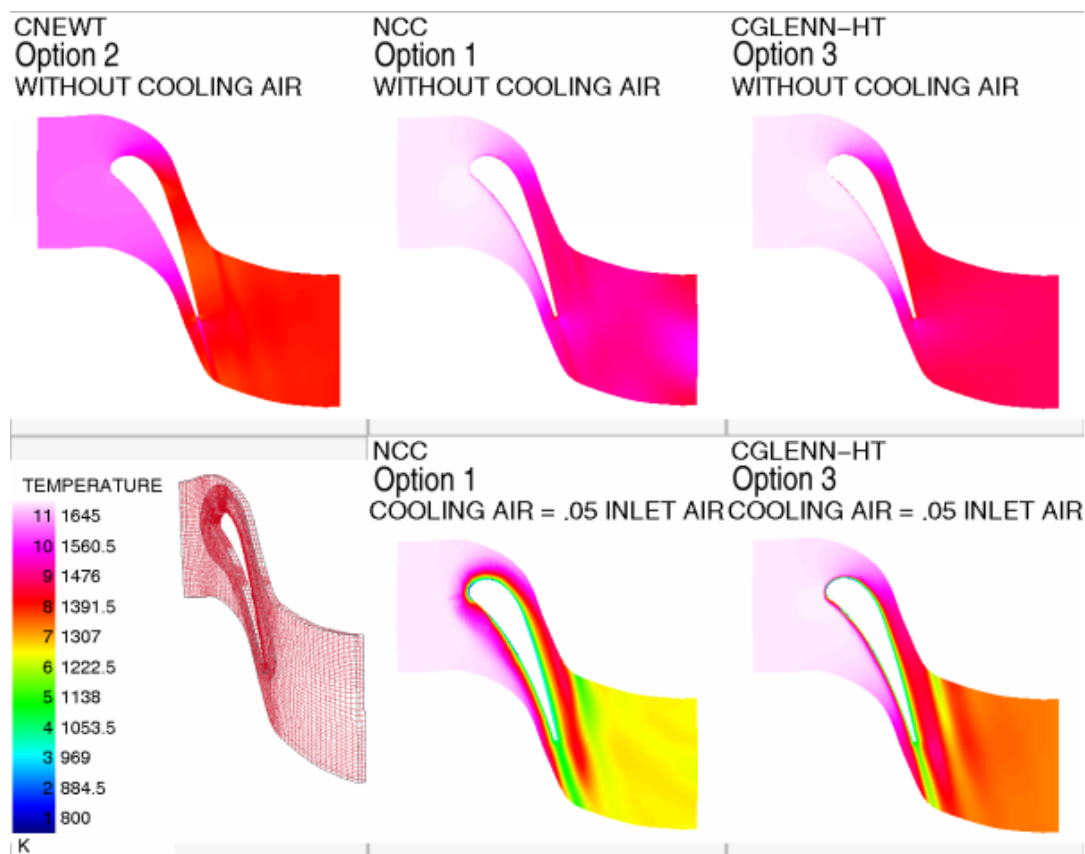


Figure 6: Comparison of temperature distributions.

The temperature contours of the results are presented in Figure 6. The temperature distributions along the axis of flow path are depicted in Figure 7. It indicates that the impact of film cooling on the temperature is significant. It also suggests that the evaluation of the transport properties affects the temperature more for the case with cooling air than the case without cooling air.

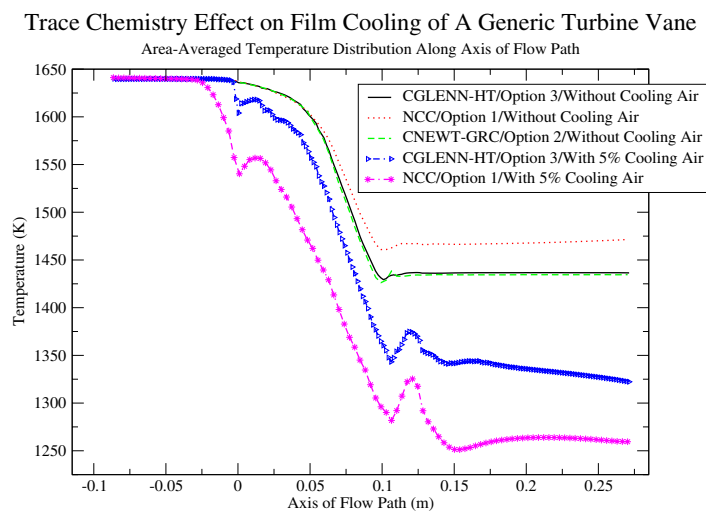


Figure 7: Comparison of area-averaged temperature distributions along the axis of flow path.

CO distributions are presented in Figure 8 and Figure 9. The mass fraction decreases as the flow passes the turbine vane with or without cooling air.

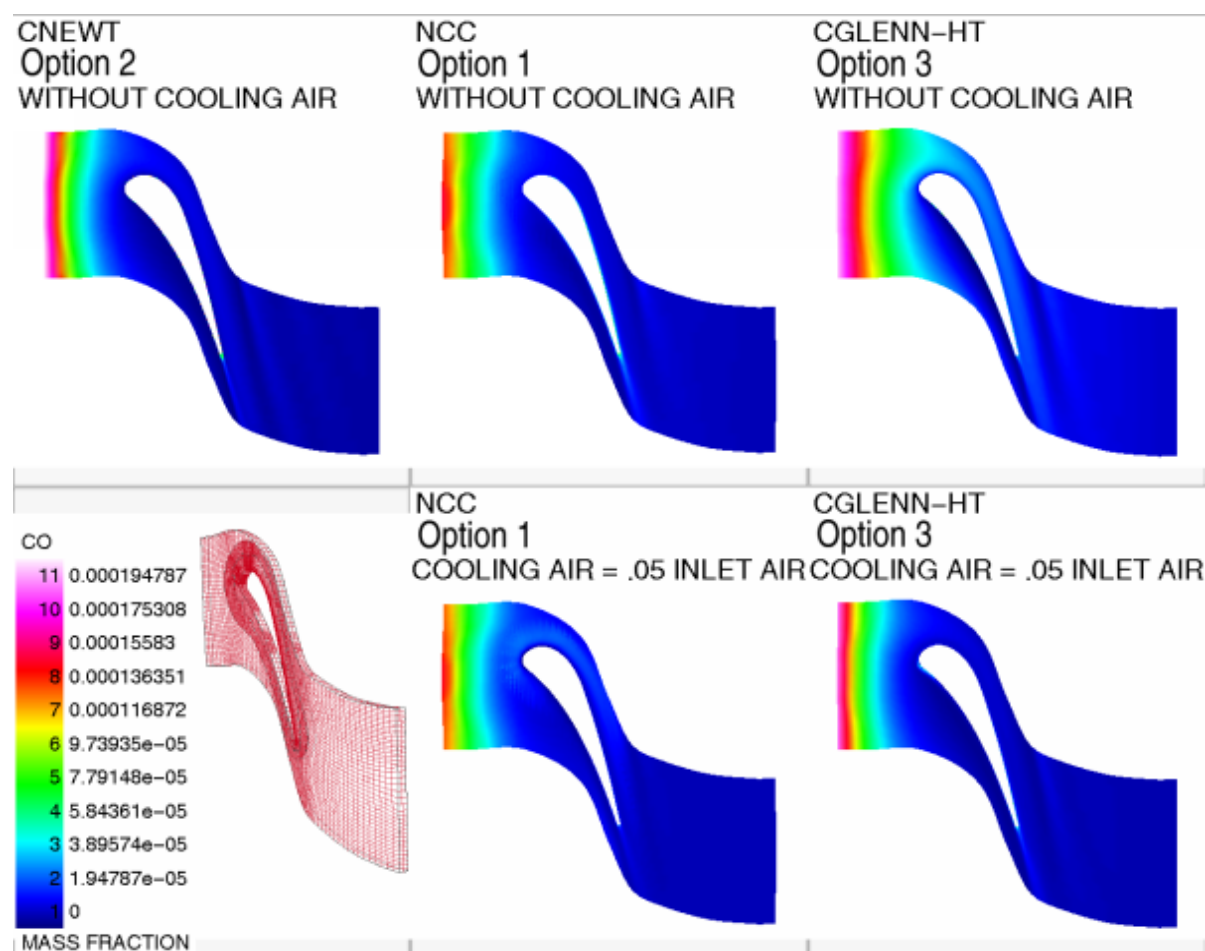


Figure 8: Comparison of CO distributions.

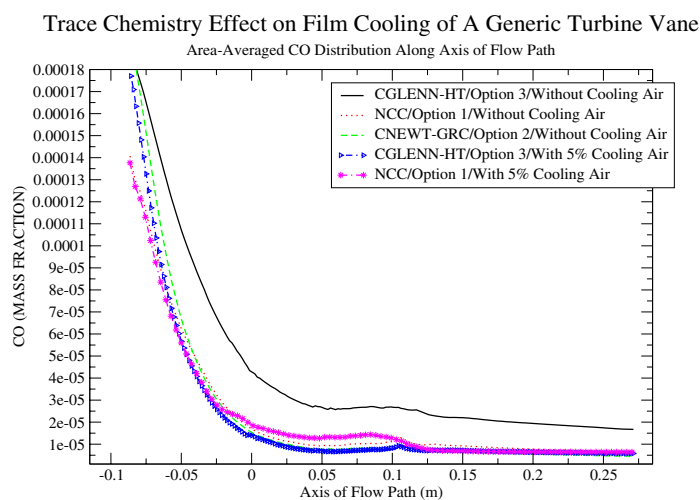


Figure 9: Comparison of area-averaged CO distributions along the axis of flow path.

NO distributions are shown in Figure 10 and Figure 11. The mass fraction for the case with cooling air decreases significantly as the flow passes the turbine vane.

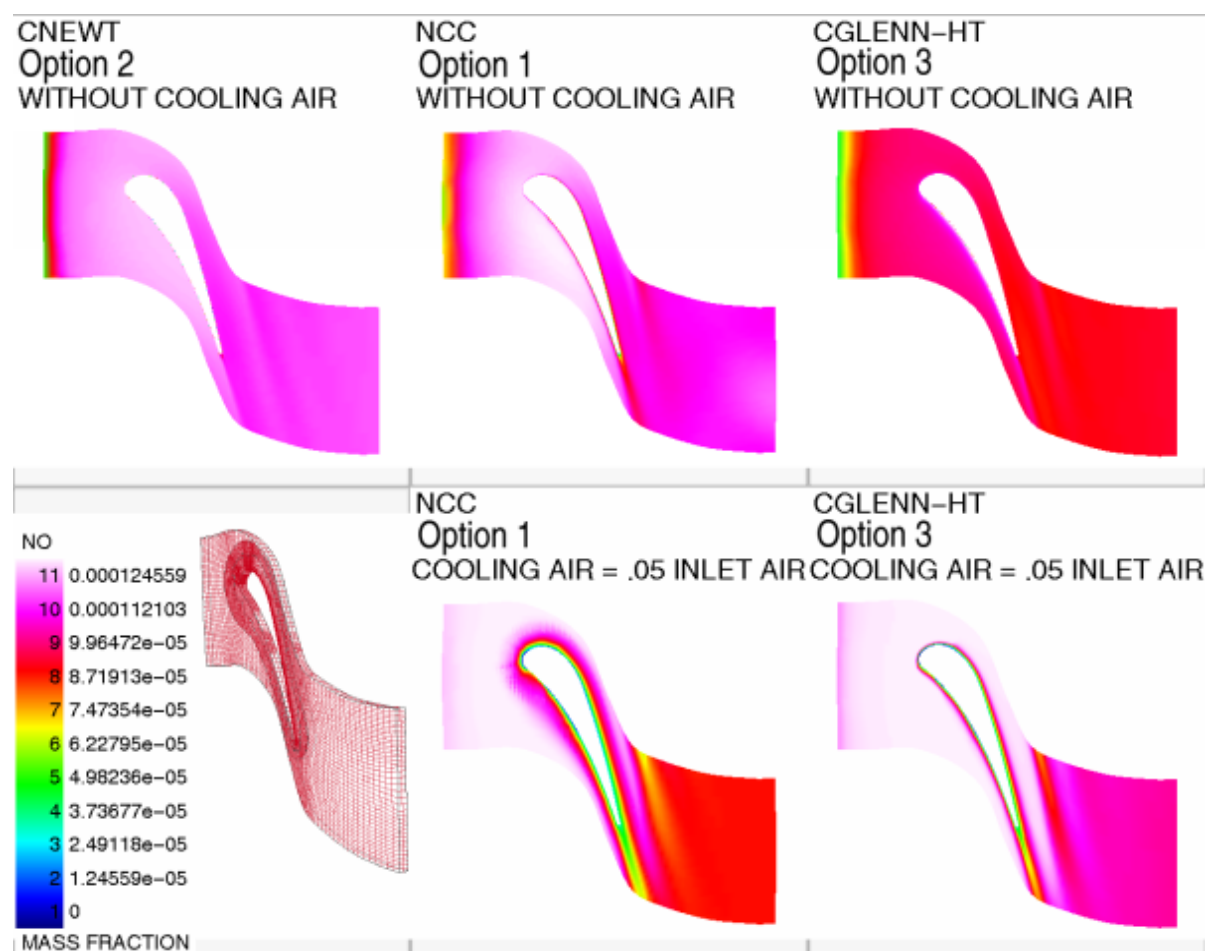


Figure 10: Comparison of *NO* distributions.

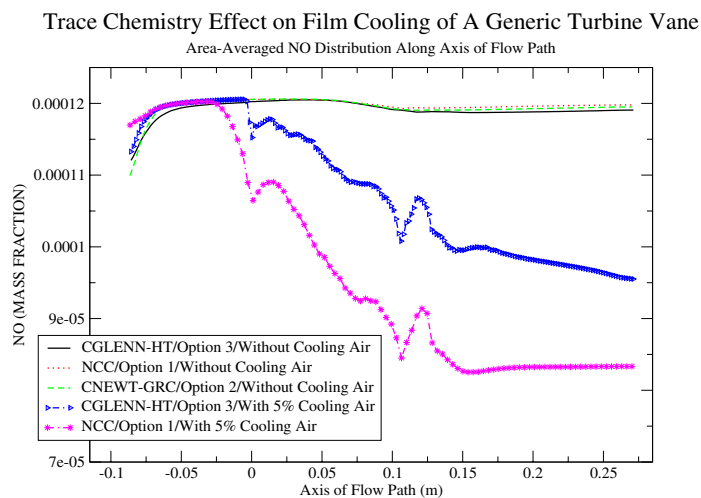


Figure 11: Comparison of area-averaged *NO* distributions along the axis of flow path.

NO_2 distributions are given in Figure 12 and Figure 13. The mass fraction with cooling air increases more than that without cooling air as the flow passes the turbine vane.

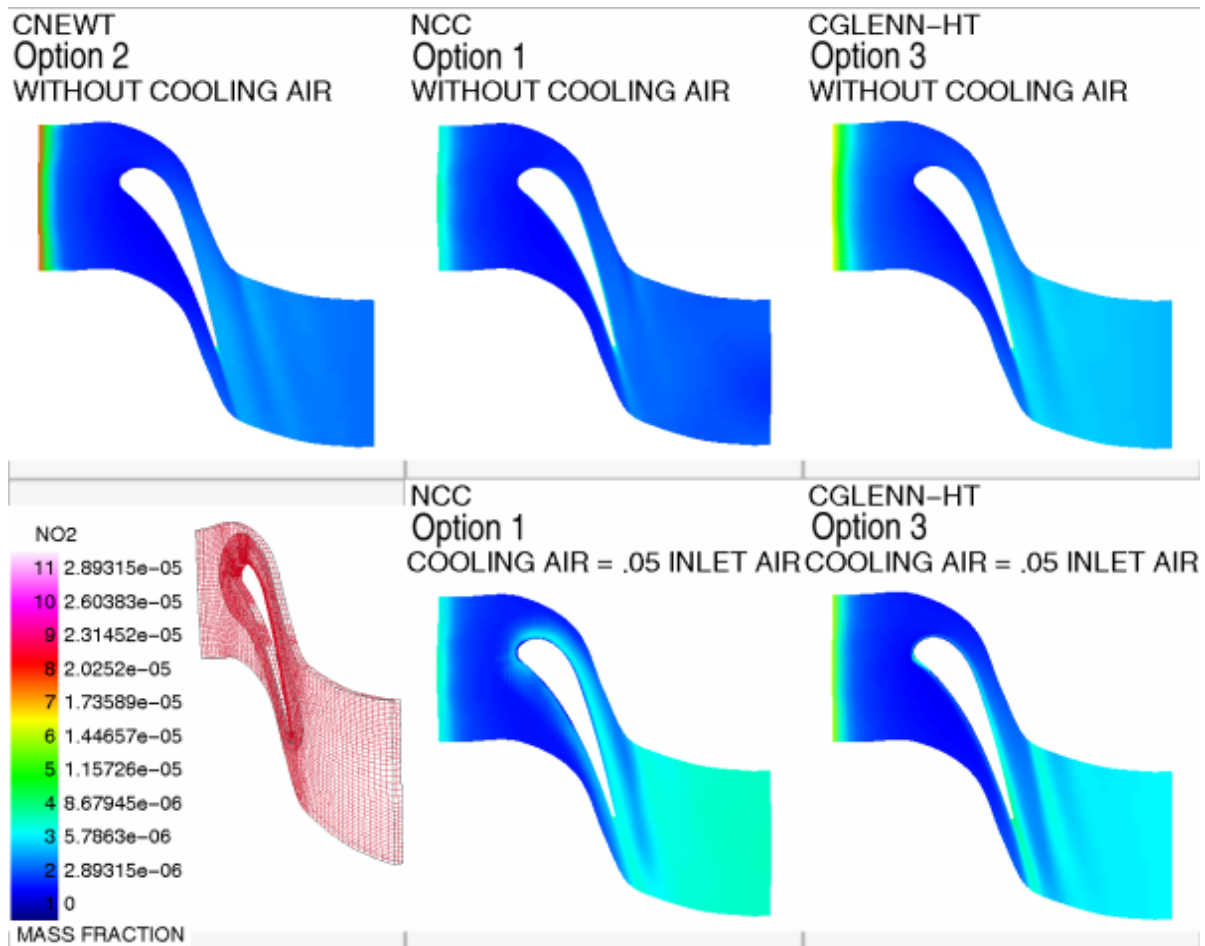


Figure 12: Comparison of NO_2 distributions.

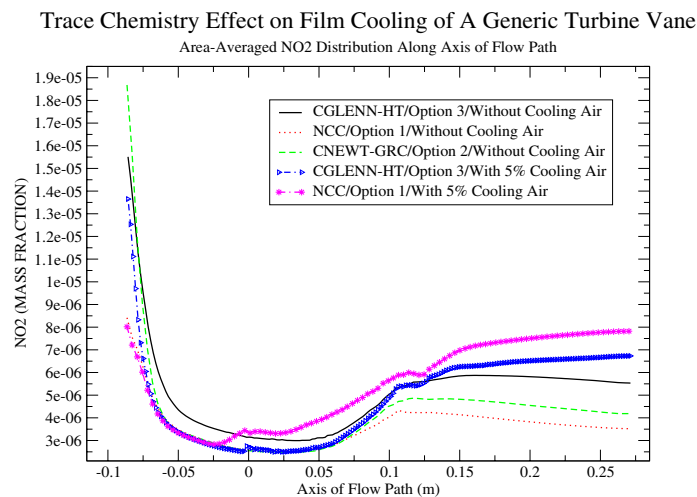


Figure 13: Comparison of area-averaged NO_2 distributions along the axis of flow path.

SO_2 distributions are shown in Figure 14 and Figure 15. The mass fraction with cooling air decreases by an amount of 25 to 30 percent of the inlet value as the flow passes the turbine vane, while the mass fraction without cooling air remains essentially the same.

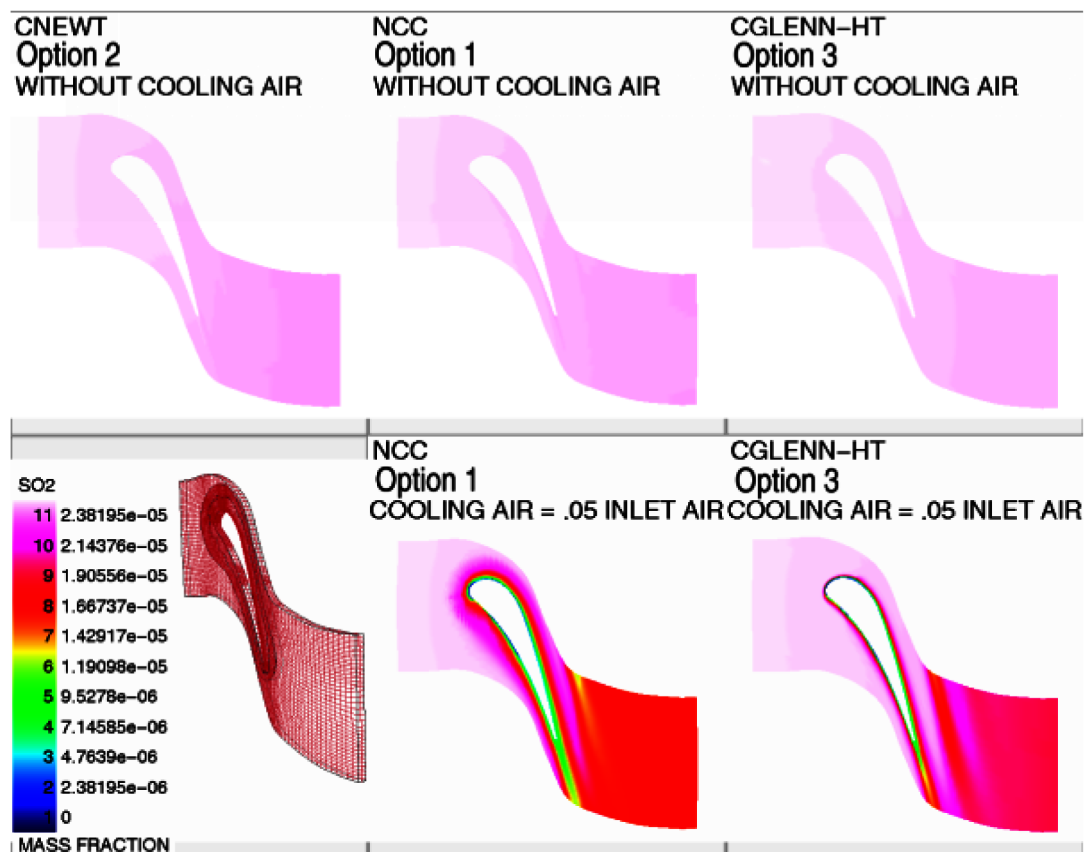


Figure 14: Comparison of SO_2 distributions.

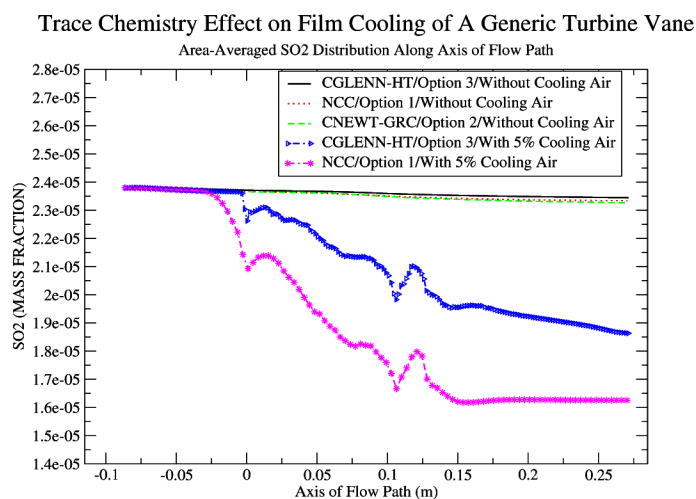


Figure 15: Comparison of area-averaged SO_2 distribution along the axis of flow path.

SO_3 distributions are presented in Figure 16 and Figure 17. The mass fraction with cooling air increases more than that without cooling air as the flow passes the turbine vane.

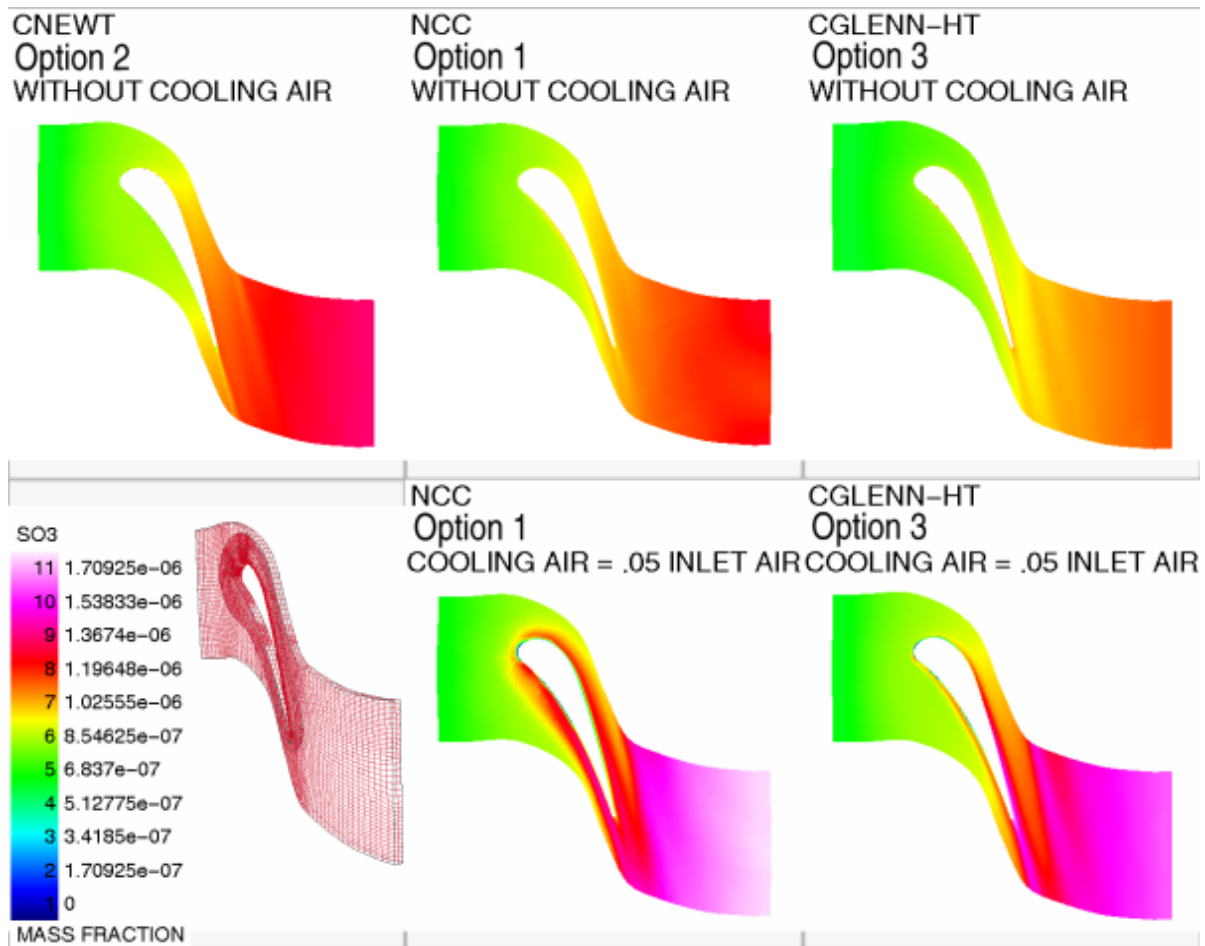


Figure 16: Comparison of SO_3 distributions.

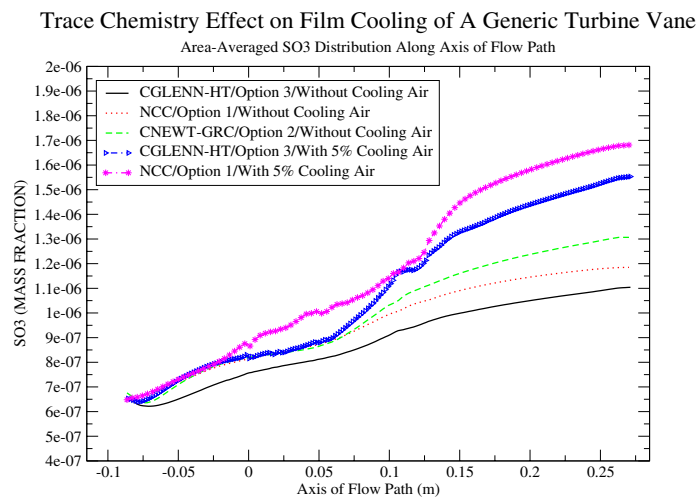


Figure 17: Comparison of area-averaged SO_3 distribution along the axis of flow path.

The area-averaged *HONO* distributions are shown in Figure 18. The mass fraction with cooling air varies more than that without cooling air.

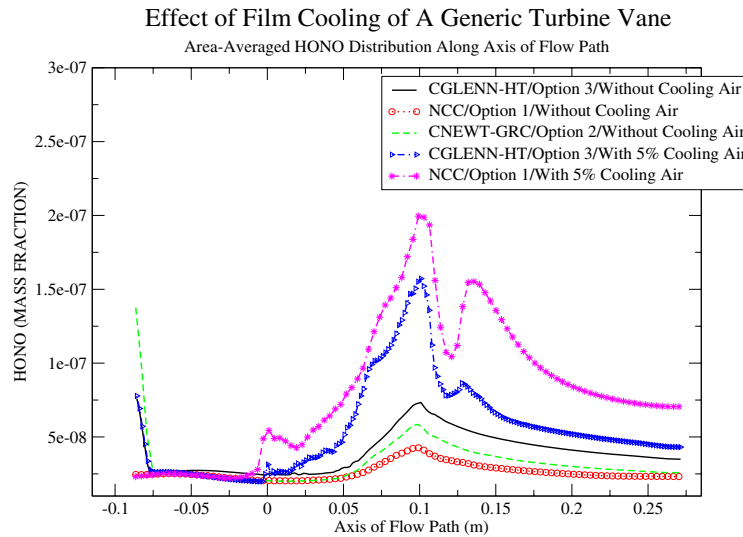


Figure 18: Comparison of area-averaged *HONO* distributions along the axis of flow path.

Figure 19 gives the area-averaged velocity distribution.

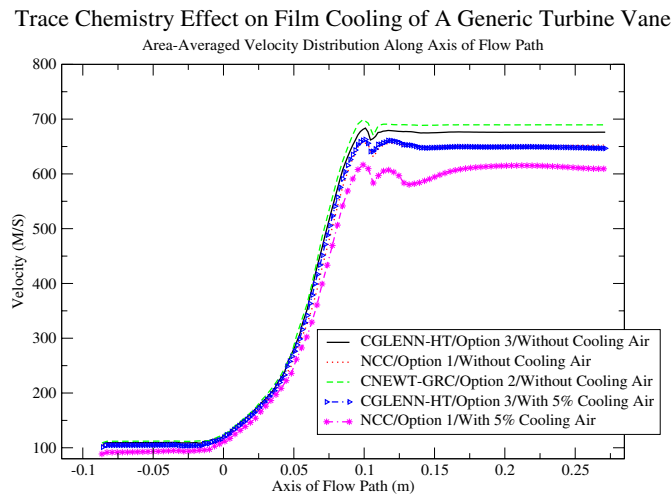


Figure 19: Comparison of area-averaged velocity distributions along the axis of flow path.

7 Concluding Remarks

- A two-dimensional representation of the 3D geometry is used for the present analysis.
- The coolant mass flow rate is about five percent of the inlet main flow.
- The present work indicates that the cooling air has an influence on the temperature and trace species mass fractions. In particular, the values of the mass fractions of *NO* and *SO₂* are lower while the mass fractions of *NO₂* and *SO₃* are higher than the corresponding values without the presence of the cooling air.
- Among other factors such as numerical schemes and turbulence models, a significant factor leading to the difference of the results obtained by NCC and CGLENN-HT is the approach for evaluating the transport properties. The effects of the heat release due to the chemical reactions are not considered in the CGLENN-HT code.
- The CGLENN-HT code was designed to run in parallel on a cluster of 2, 3, 4, 5, 6 or 12 nodes using MPICH, a freely available implementation of the MPI (message passing interface) standard. Only the chemistry subroutines of CGLENN-HT are parallelized. The NCC code was designed to run in parallel on a cluster of arbitrary number of nodes using MPICH. The entire code is parallelized based upon the principle of the domain decomposition. Thus wall clock time of computation using the NCC code can be significantly reduced by requesting more computer nodes, while the CGLENN-HT is much more limited in this respect. For the film cooling cases running NCC and CGLENN-HT on the LOMAX machine of the NAS facility, the run time statistics is
 - NCC — On a single node, the average wall clock time is about 120 second per iteration. It can achieve a speedup in an almost linear fashion by adding more CPU's. For example, on 32 nodes, the average wall clock time is about 3.75 second per iteration.
 - CGLENN-HT — On a single node, the average wall clock time is about 80 second per iteration. The average wall clock time is about 59 second per iteration on two nodes, 46 second per iteration on three nodes, 41 second per iteration on four nodes and 39 second per iteration on six nodes.

This speedup limitation of the CGLENN-HT code is taken into consideration, as we decide to use NCC for furthering the post-combustion chemistry modeling and simulations.

References

- [1] Thomas Wey and Nan-Suey Liu, "Current Status of Post-Combustor Trace Chemistry Modeling and Simulation at NASA GRC", Sept. 2002, submitted for publication as a NASA TM.

- [2] James D. Heidmann, David L. Rigby and Ali A. Ameri, "A Three-Dimensional coupled Internal/External Simulation of a Film-Cooled Turbine Vane," ASME J. Turbomachinery, Vol. 122, pp.348-359, April 2000.
- [3] Thomas C. Wey, "Development of A Mesh Interface Generator For Overlapped Structured Grids", AIAA 94-1924, AIAA 12th Applied Aerodynamics Conference, June 20-22, 1994/Colorado Spring, CO.
- [4] S. P. Lukachko, I. A. Waitz, R. C. Miake-Lye, R. C. Brown and M. R. Anderson, "Production of Sulfate Aerosol Precursors in The Turbine and Exhaust Nozzle of An Aircraft Engine," Journal of Geophysical Research Vol.103, NO.D13, Pages 16.159-16.174, July 20, 1998.

REPORT DOCUMENTATION PAGE			Form Approved OMB No. 0704-0188	
Public reporting burden for this collection of information is estimated to average 1 hour per response, including the time for reviewing instructions, searching existing data sources, gathering and maintaining the data needed, and completing and reviewing the collection of information. Send comments regarding this burden estimate or any other aspect of this collection of information, including suggestions for reducing this burden, to Washington Headquarters Services, Directorate for Information Operations and Reports, 1215 Jefferson Davis Highway, Suite 1204, Arlington, VA 22202-4302, and to the Office of Management and Budget, Paperwork Reduction Project (0704-0188), Washington, DC 20503.				
1. AGENCY USE ONLY (Leave blank)		2. REPORT DATE January 2003		3. REPORT TYPE AND DATES COVERED Technical Memorandum
4. TITLE AND SUBTITLE Film Cooling Flow Effects on Post-Combustor Trace Chemistry			5. FUNDING NUMBERS WBS-22-714-01-13	
6. AUTHOR(S) Thomas Wey and Nan-Suey Liu				
7. PERFORMING ORGANIZATION NAME(S) AND ADDRESS(ES) National Aeronautics and Space Administration John H. Glenn Research Center at Lewis Field Cleveland, Ohio 44135-3191			8. PERFORMING ORGANIZATION REPORT NUMBER E-13722	
9. SPONSORING/MONITORING AGENCY NAME(S) AND ADDRESS(ES) National Aeronautics and Space Administration Washington, DC 20546-0001			10. SPONSORING/MONITORING AGENCY REPORT NUMBER NASA TM-2003-212018	
11. SUPPLEMENTARY NOTES Thomas Wey, Taitech, Inc., Beavercreek, Ohio 45430; Nan-Suey Liu, NASA Glenn Research Center. Responsible person, Nan-Suey Liu, organization code 5830, 216-433-8722.				
12a. DISTRIBUTION/AVAILABILITY STATEMENT Unclassified - Unlimited Subject Category: 07 Available electronically at http://gltrs.grc.nasa.gov This publication is available from the NASA Center for AeroSpace Information, 301-621-0390.			12b. DISTRIBUTION CODE	
13. ABSTRACT (Maximum 200 words) Film cooling injection is widely applied in the thermal design of turbomachinery, as it contributes to achieve higher operating temperature conditions of modern gas turbines, and to meet the requirements for reliability and life cycles. It is a significant part of the high-pressure turbine system. The film cooling injection, however, interacts with the main flow and is susceptible to have an influence on the aerodynamic performance of the cooled components, and through that may cause a penalty on the overall efficiency of the gas turbine. The main reasons are the loss of total pressure resulting from mixing the cooling air with mainstream and the reduction of the gas stagnation temperature at the exit of the combustion chamber to a lower value at the exit of nozzle guide vane. In addition, the impact of the injected air on the evolution of the trace species of the hot gas is not yet quite clear. This work computationally investigates the film cooling influence on post-combustor trace chemistry, as trace species in aircraft exhaust affect climate and ozone.				
14. SUBJECT TERMS Film cooling; Emission			15. NUMBER OF PAGES 21	
			16. PRICE CODE	
17. SECURITY CLASSIFICATION OF REPORT Unclassified	18. SECURITY CLASSIFICATION OF THIS PAGE Unclassified	19. SECURITY CLASSIFICATION OF ABSTRACT Unclassified	20. LIMITATION OF ABSTRACT	